High frequency electro-optic measurement of strained silicon racetrack resonators

M.BORGHI[1,*], M.MANCINELLI[1], F.MERGET[2], J.WITZENS[2], M.GHULINYAN[3], G.PUCKER[3], AND L.PAVESI[1]

[1] Department of Physics, Nanoscience Laboratory, University of Trento, I-38123 Povo, Italy
[2] Institute for Integrated Photonics, RWTH Aachen University Sommerfeldstr. 24, D-52074, Aachen, Germany
[3] Centro Materiali e Microsistemi, Bruno Kessler Foundation, I-38123 Povo, Italy
[*] Corresponding author: massimo.borghi@unitn.it

Compiled September 7, 2015

The observation of the electro-optic effect in strained silicon waveguides has been considered a direct manifestation of an induced χ^2 non-linearity in the material. In this work, we performed high speed measurements on strained silicon racetrack resonators. Strain is controlled by a mechanical deformation of the waveguide. It is proved that any optical modulation vanishes independently from the applied strain when the applied voltage varies much faster than the carrier lifetime. This demonstrates that plasma carrier dispersion is responsible of the observed electro-optic effect. Our results set an upper limit of $3\,pm/V$ to the induced χ^2_{zzz} tensor element at an applied stress of 0.5 GPa. This upper limit is more than one order of magnitude lower than the previously reported values for static electro-optic measurements.

OCIS codes: *(130.4110) Integrated Optics, modulators; (130.3130) Integrated Optics, integrated optics materials.*

http://dx.doi.org/10.1364/ao.XX.XXXXXX

1. INTRODUCTION

In the last years, a lot of effort was spent to search for the strain induced second order nonlinearity (χ^2 effect) in silicon by looking at the Pockel effect [1–5]. Strain induced χ^2 would be instrumental to make ultrafast and energy efficient electro-optic modulators for the silicon photonics platform which would replace present electro-optic modulator based on plasma dispersion effect [6–10]. More generally, the presence of an appreciable χ^2 in silicon would validate the Silicon-on-Insulator (SOI) platform as an alternative to Lithium Niobate for second order nonlinear optics [11, 12]. In most of these works, the centro-symmetry of Silicon is broken by a stressing film of Silicon-Nitride which strain the underlying Silicon waveguide and enable a $\chi^2 \neq 0$ - at least from a mathematical point of view [13]. With the exception of refs. [11, 12], the Pockel effect was investigated by using an integrated Mach-Zehnder interferometer in which one or both interferometer arms are driven by a DC or a low frequency ($\approx kHz$) AC electric field [1–5]. Then, an effective χ^2 value is extracted from a measured shift of the interference fringes by knowing the system geometry and the amount of the applied static electric field. As expected from the theory, the relation between the effective index change and the applied static electric field is found to be linear. The linear relation between these two physical quantities is advocated as *the* evidence of the observation of a Pockel effect. Unfortunately, a linear effective index variation of the optical mode of a waveguide can be also induced by free carriers [14, 15] or by traps states and localized charges at the SiN_x-Si interface [12, 14]. A definitive prove or disprove of the strain induced non-linearity can be obtained by high frequency measurements in an interferometer structure since Pockel effects or free carrier dispersion are characterized by two different characteristic times.
In this letter, we aim to measure the separate contributions to the effective χ^2 of the Pockel effect and of the plasma dispersion effect. We investigate the frequency response of the electro-optic effect in a racetrack resonator up to $5\,GHz$, i. e. well above the free carriers lifetime in the waveguide. In particular, by using a dedicated set-up, we were able to tune continuously the strain in a same device so to verify accurately how the applied strain modifies the system frequency response.

2. DEVICE AND EXPERIMENTAL SETUP

Our test structure is shown in Figure 1(a). It is a racetrack resonator in the Add-Drop filter configuration [16] fabbricated on a 6′ SOI wafer. The resonator has a perimeter of $415\,\mu m$ and a coupling coefficient with the bus waveguide of $\kappa^2 = 7\%$. A $140\,nm$ thick LPCVD Silicon Nitride (SiN_x) layer is conformally grown on the silicon waveguide. The residual strain on the SiN_x layer has been measured to be $-0.19\,GPa$. We used a $2.5\,\mu m$ thick Buried Oxide Layer (BOX) and a $900\,nm$ thick Silica layer as lower and upper cladding materials. An electric field can be applied in the z direction using three Aluminum electrodes along a $50\,\mu m$ straight waveguide section. The waveguide width changes adiabatically from $400\,nm$ outside the electrodes to $1600\,nm$ under them. The height is kept fixed to $250\,nm$. Using the adiabatic tapers, we are able to probe the electro-optic modu-

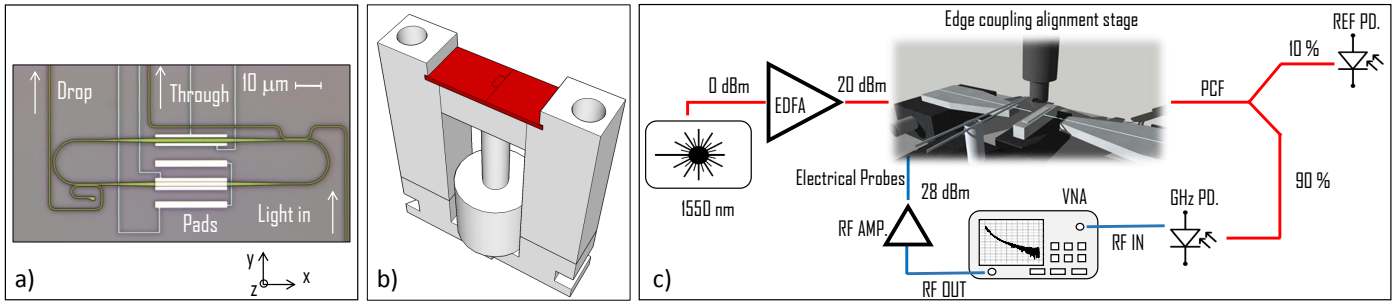

Fig. 1. (a) Optical microscope image of the racetrack resonator. (b) A 3D model of the stressing sample holder. The sample is indicated in red. (c) Experimental setup used for the electro-optic measurements. PCF = Polarization Maintaining Fibers, PD = Photodiodes, VNA = Virtual Network Analyzer, RF IN(OUT) = Radio Frequency IN(OUT).

lation on the 1600 nm wide multimode waveguide by preserving the fundamental mode excitation. As shown in fig. 1(b), the device is fixed on a sample holder which can provide a variable stress by rotating a 250 μm pitch screw. The material strain is mechanically induced by fixing the sample ends to the holder and then by bending its center though the pressure exercised by the top of the screw. We found that it is possible to displace the screw of approximately its complete pitch before breaking the chip. To avoid micro fractures, we kept screw displacements lower than 150μm. Note that, at odds with the other works where the strain is changed by using various samples[1–5, 11, 12], with this method it is possible to tune continuously the strain in a same resonator. As indicated in fig. 1(c), light from a C-band infra-red laser amplified by a Erbium Doped Fiber Amplifier (EDFA) is edge coupled to the Input port of the resonator using a Polarization Maintaining lensed Fiber (PMF). The light polarization is set to Transverse Magnetic (TM). A nanometric XYZ positioning stage is used to minimize the coupling losses. The transmitted light from the resonator Through port is split: 10% is sent to a reference photodiode, while 90% feeds a high bandwidth photoreceiver (43 GHz) connected to a Virtual Network Analyzer (VNA). The VNA provides also 28 dBm of sinusoidal voltage modulation to the electrodes using impedance matched Tungsten tips of 40 GHz bandwidth.

3. METHODS AND DISCUSSION OF RESULTS

A. Evaluation of the stress level inside the waveguide

In order to get a quantitative relation between stress inside the waveguide and the screw displacement, we used a Finite Element Method (FEM) computation. The results are shown in Figure 2(a-b). Only the s_{xx} element of the stress tensor s_{ij} is plotted, since it is found to be one order of magnitude higher than the s_{yy} component and five orders of magnitude higher than the remaining tensor elements. In the region where the resonator is located (dashed rectangle in Figure 2(a)), the global stress distribution can be considered as tensile and uni axial in the x direction. In Figure 2(b), we show a linear relation between the screw displacement and the computed average stress in the waveguide. At our working point (displacement $\approx$ 150 μm), the stress level is about 0.48 GPa in the waveguide and 0.78 GPa in the SiN_x layer. These values are comparable to the one used in other experiments [1–5, 11, 12]. In the inset of fig. 2(a) we also notice that a high stress (hence strain) gradient is present at the upper and lower interfaces between SiN_x and the waveguide. This feature is essential since it is theoretically predicted that the

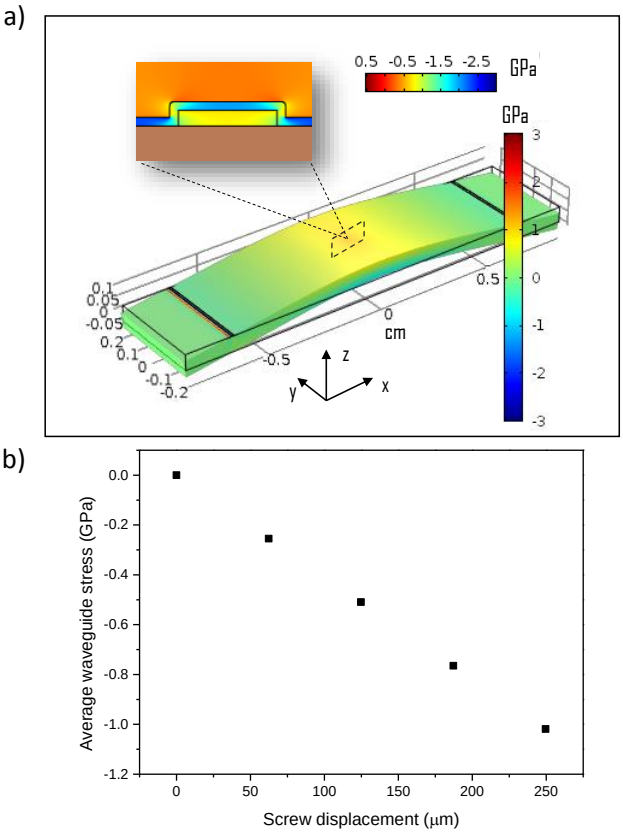

Fig. 2. (a) Finite Element simulation of the stress distribution (s_{xx} element of the stress tensor s_{ij}) on the sample subjected to a 62.5 μm screw displacement. The discontinuities near the ends are due to the line contact with the sample holder (see fig. 1(b)), which lies 2 mm far from the ends. The inset shows the stress profile along the waveguide cross section. (b) Average stress (s_{xx}) inside the waveguide as a function of the screw displacement.

induced χ^2 is proportional to the strain gradient in the material [11, 13].

B. Frequency behaviour of the optical modulation

At first, we set the screw displacement to zero, so no stress (except the residual one due to $SiN_x - Si$ interface) is applied to the waveguide. By monitoring the output signal at the reference

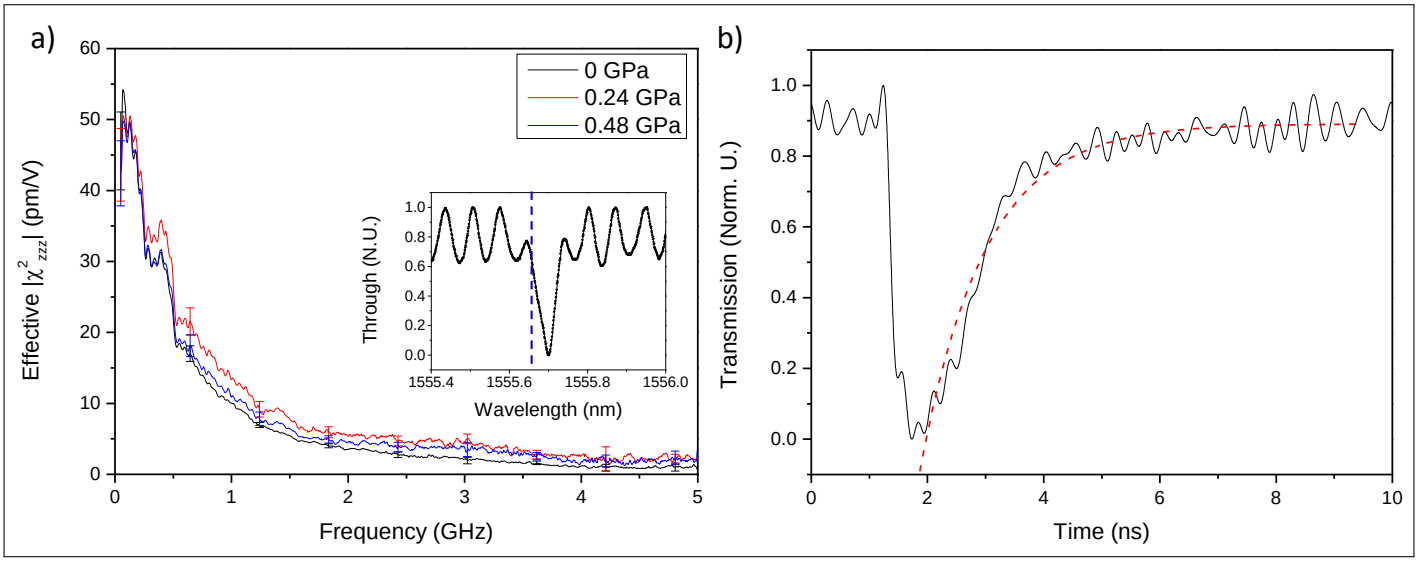

Fig. 3. (a) Effective χ^2 as a function of the electrical modulation frequency for three different stress levels in the waveguide. For clarity, the errors are reported only for certain points of the curves. The inset shows the working point of the electro optic measurement. The black line denotes the Through transmission while the vertical blue dashed line represents the wavelength of the laser. (b) Measurement of the carrier lifetime. The black line is the Drop signal (in normalized units) in time while the red dotted line is an exponential fit of the raising edge.

photodiode (fig. 1(c)), we tuned the laser wavelength near the $-3dB$ point of one of the resonances (fig. 3 (a) inset), where the sensitivity to small refractive index variations is maximum. The quality factor of this resonance is $Q \approx 23200$. We then applied a sinusoidal voltage to the sample electrodes (fig. 1 (a)) using the VNA and a $32\,dB$ electrical amplifier. As a result of the bias modulation, the resonance oscillates back and forth with respect to the laser wavelength, inducing a periodic modulation of the transmitted optical signal at the Through port of the resonator. Assuming that this signal modulation is due to the electro-optic effect caused by the strain induced second order nonlinearity, we model the modulation and, from the data, we extract an effective χ^2_{zzz}. Figure 3(a) shows the effective χ^2_{zzz} values as a function of the driving bias frequency. The voltage frequency is swept from $50\,MHz$ to $5\,GHz$. As we can see, the value of χ^2_{zzz} is maximum in the low frequency range, and decreases as the modulation frequency increases. We point out that the χ^2_{zzz} value in the nearly DC regime is $\approx 50\,pm/V$, which is comparable to the ones found in the literature for static electro-optic measurements [3, 4]. The cut-off frequency, i.e the frequency at which the χ^2_{zzz} halves, is $\nu_c = (0.50 \pm 0.01)\,GHz$, corresponding to a period of $\tau = (2.00 \pm 0.04)\,ns$. The minimum value of χ^2_{zzz} that can be detected is limited by the electrical noise floor of the VNA and of the photoreceiver. This corresponds to an effective χ^2_{zzz} of $\approx 3\,pm/V$. By looking at Fig. 3(a), this value is reached for $\nu \geq 4.5\,GHz$. To exclude the possibility that the bandwidth is limited by the photon lifetime in the cavity, we modulated the optical input, and then we measured the signal at the Drop port when the laser wavelength is tuned on resonance. The signal drops by $\approx -1.3\,dB$ from $50\,MHz$ to $5\,GHz$, showing that the cavity is far from the optical cut-off. This frequency response has been subtracted to the curves in Figure 3(a).

As shown in Fig. 3(a), we repeated the electro-optic measurement by applying a stress to the waveguide of $0.24\,GPa$ and $0.48\,GPa$. Negligible differences are observed with respect to the no-stress case. We also tested waveguides with smaller widths, such as $400\,nm$ and $800\,nm$, and found smaller transmission signal modulations compared to the $1600\,nm$ wide one.

These results clearly show that the modulation can not be attributed to a strain induced χ^2, e.g. to the linear electro-optic effect. In fact, if this would be the case, the trasmitted signal should follow the voltage variations instantaneously up to optical frequencies. The signal modulation is rather related to a slower dispersion mechanism, with a characteristic time in the nanosecond time range. It has been recently shown that the plasma carrier dispersion effect can behave as a linear electro-optic modulation if a charge layer is present at the SiN_x-Si interface [14**?**]. Therefore, we checked the carrier lifetime in our waveguide to verify its consistency with the cut-off frequency in the electro-optic experiments. We used a pump and probe scheme, where an intense ps laser pulse is coupled to the waveguide and the time dependent losses of a weaker probe beam are monitored. The short pump pulse generates free carriers due to two-photon absorption (TPA), these free carriers in turn attenuates the probe signal due to free-carrier absorption. After the switch off of the pump laser, the probe beam transmission slowly recovers due to free carrier recombinations. Through the measurements of the recovery of the probe beam, the free carrier recombination lifetime can be measured. The result is shown in fig. 3(b). The sudden signal decrease is due to the pulse arrival and, consequently, to TPA carrier generation. The following slower signal raise is due to free carrier recombination. From these data, we estimated a carrier lifetime of $\tau_c = (1.06 \pm 0.01)\,ns$. Being $\tau_c \simeq 1/\nu_c$, we conclude that the observed modulation can be attributed to plasma carrier dispersion. As a further support, we applied static DC voltages to the electrodes of the racetrack resonator. We swept from $0\,V$ to $70\,V$, and we measured the Drop port transmitted signal as a function of the bias. We found that the Drop transmission signal monotonically decreases with voltage, reaching a minimum value of $-1\,dB$ with respect to the zero bias condition. This behavior confirms that the electro-optic modulation is actually induced by free carriers. What is more

interesting is the observation that the modulation frequency response is limited by the carrier recombination rate. Therefore, the waveguide refractive index change is not induced by the electron-hole redistribution as a response to the applied voltage. Indeed, such phenomena are speed-limited by the electron-hole mobility and have cut-off frequencies above few GHz [9, 10]. A plausible explanation of our observations is the accumulation and release of carriers at the SiN_x-Si interfaces as a consequence of the applied voltages [14, 17, 18].
In addition, we set an upper limit to the strain induced χ^2_{zzz} of $3\,pm/V$ at 0.5 GPa of applied stress. This value is more than an order of magnitude lower than those reported for the DC regime measurements [2–5], where we believe that the χ^2 induced modulations are completely masked by free carrier effects. We remark here that, with our work, we do not exclude the presence of a strain induced χ^2 in Silicon. Indeed, there exist proofs of second order harmonic generation in strained Silicon that intrinsically can not have a free carrier interpretation [11, 12, 19]. These experiments revealed a χ^2 value of up to $40\,pm/V$ for 1.2 GPa applied stress. Differences can be due to the fact that the χ^2 tensor is dispersive, so its value at optical frequencies can be significantly different from the one measured at DC [11].

4. CONCLUSION

In this work, we demonstrated that a strong linear electro-optic effect is present in strained Silicon waveguides due to free carrier dispersion. A dedicated experimental set-up allows us continuously tuning the applied stress on a very same racetrack resonator. By performing high frequency measurements of the optical transmission under an AC electric field variation, we found that the electro-optic modulation vanishes as the modulation speed exceeds the free carrier lifetime. Thus, we evidenced a non-instantaneous time response and, consequently, we ruled out the potential ultrafast χ^2 origin of the modulation. We set an upper limit of $3\,pm/V$ to the strain induced χ^2_{zzz} in Silicon waveguides, which corresponds to our minimum detectable signal. This value is more than one order of magnitude lower than the one reported in the low frequency regime in the literature, which allows us concluding that free carriers are the responsible of the observed behavior. Larger stresses or different stressing materials than SiN_x are needed to definitely prove the presence of the electro-optic effect in strained Silicon waveguide.

METHODS

Extracting the χ^2 value from the amplitude modulation

The signal intensity at the output of the Through port of the resonator I_{out} is governed by the differential equation:

$$\frac{dI_{out}(\lambda, \lambda_0(V(t)))}{dt} = \frac{\partial I_{out}}{d\lambda_0}\frac{\partial \lambda_0}{dV}\frac{dV}{dt} \quad \textbf{(1)}$$

where λ_0 is one of the resonance wavelength of the resonator. Its value can be perturbed by its value at $V = 0$ ($\bar{\lambda_0}$) by the linear electro optic induced effective change Δn:

$$\lambda_0(V) = \bar{\lambda_0}\Big(1 + \frac{\Delta n(V)}{n}\Big) \quad \textbf{(2)}$$

The change in the refractive index is related to the effective χ^2 value and the applied sinusoidal voltage $V(t) = V_0 \sin(\omega t)$ through [4]:

$$\Delta n = \frac{\chi^2_{eff} L}{2 L_{tot} n}\Big(\frac{dE}{dV}\Big) V \quad \textbf{(3)}$$

in which L is the length of region where the field is applied, L_{tot} is the resonator length, n is the effective index of the propagating mode and dE/dV is the derivative of the electric field with respect to the applied voltage, evaluated at the zero bias point ($V = 0$). By combining together Eqs.(1-3), we found that the output signal I_{out} is given by $I_{out}(t) = I_0 \sin(\omega t)$, where the amplitude I_0 is given by:

$$I_0 = \frac{\chi^2_{eff} L \bar{\lambda_0} n}{2 L_{tot} V_0}\Big(\frac{dE}{dV}\Big)\Big(\frac{dI_{out}}{d\lambda_0}\Big) \quad \textbf{(4)}$$

The amplitude I_0 is what is actually recorded by the VNA. The value of $dI_{out}/d\lambda_0$ is extracted from the spectral response (inset in Fig.3(a)), while n and dE/dV from FEM simulations. From the knwledge of these parameters and from Eq.(4) we can extract the value of χ^2_{eff}.

ACKNOWLEDGMENTS

Acknowledgment. The authors acknowledge Dr.Saeed Sharif for the collaboration and useful discussions we had during the measurement sessions. This work has been supported by the SIQURO project financed by the Autonomous Provincia of Trento.

REFERENCES

1. S.R. Jacobsen et al, Nature, **441**, 199-202, (2006).
2. B. Chmielak et al., Opt. Express, **21**, 25324-25332, (2013).
3. B. Chmielak et al, Opt. Express, **19**, 17212-17219, (2011).
4. M. W. Puckett et al., Opt. Letters, **39**, 1693-1696, (2014).
5. P.Damas et al, Opt. Express, **22**, 22095-22100, (2014).
6. G. T. Reed et al., Nature Phot., **4**, 518-526, (2010).
7. M. Ziebell et al., Opt. Express, **20**, 10591-10596, (2012).
8. Q. Xu et al, Nature, **435**, 325-327, (2005).
9. A.Liu et al, Nature, **427**, 615-618, (2004).
10. A.Liu et al., Opt. Express, **15**, 660-668, (2007).
11. M. Cazzanelli et al., Nature Materials, **11**, 148-154, (2012).
12. S.Clemens et al., Advanced Optical Materials, **3**, 129-136, (2015).
13. C. Manganelli, P. Pintus, and C. Bonati., arXiv preprint, arXiv:1507.06589 (2015).
14. S.S. Azadeh et al., Opt. Letters, **40**, 1877-1880, (2015).
15. R. Sharma et al., Appl. Phys. Lett. **106**, 241104 (2015).
16. M.Masi et al., Journal of Lightwave Technology, **28**, 3233-3242, (2010).
17. P. Zhang et al., Nature, **439**, 703-706, (2006).
18. L. Alloatti, C. Koos, and J. Leuthold, Appl. Phys. Lett., **107**, 031107 (2015)
19. S.V. Govorkov et al., J. Opt. Soc. Am. B, **6**, 1117-1124, (1989).